International Journal of Industrial Engineering & Production Research September 2020 Vol. 31, No. 3: 409-422
DOI: 10.22068/ijiepr.31.3.409

RESEARCH PAPER

Investigation of Laser Engraving Qualitative Characteristics of Al-SiC Composite Using Design of Experiments

Rassoul Noorossana*[1], Mahdi Shayganmanesh[2], Farhad Pazhuheian[3] & Mohammad Hosein Rahimi[4]

Received 18 May 2018; Revised 8 May 2019; Accepted13 July 2020; Published online 30 September 2020

ABSTRACT
Laser marking is an advanced technology in material processing that has a permanent effect on materials. The materials are removed layer by layer via laser engraving in the laser path through melting displacement, ablation, and evaporation. Al-SiC is a metal matrix composite that is widely used in aerospace, automobile manufacturing, and electronic packaging. Accumulative Roll Bonding (ARB) is one of the newest manufacturing processes of metal matrix composites which finally produces materials with high strength, low weight, and great environmental compatibility. This study investigates the laser engraving of Al-SiC composite samples which are produced through ARB process by using Q-switched Nd:YAG laser. In this study, the 2k factorial design was used to analyze the effects of factors, including assistant gas flow, sample distance from beam focus location (distance), pulse repetition frequency, and pumping current on the qualitative characteristics of engraved zone (width, depth, and contrast of engraved zone). Desirability function was also used for optimization. The results that were based on experimental data indicated the optimal setting of input factors, leading to pre-specified target values of responses.

KEYWORDS: *Laser engraving; Al-SiC composite; Accumulative roll bonding; 2k design; Desirability function.*

1. Introduction

Laser processing techniques enjoy high speed, accuracy, and flexibility and are appropriate for cutting, marking, drilling, and micromachining in most materials such as metals, plastics, ceramics, and composites [1]. The most common types of lasers that are appropriate for manufacturing processes are pulsed Nd:YAG lasers and continuous CO_2 lasers. The pulsed Nd:YAG lasers are appropriate for machining processes due to several advantages such as high intensity and small spot size. Laser machining is a complex dynamic process, affected by numerous parameters which need to be precisely controlled [2]. As an illustration, Fig.1 shows a schematic representation of laser marking process.

* **Corresponding author:** ***Rassoul Noorossana***
rassoul@iust.ac.ir

1. *Industrial Engineering Department, Iran University of Science and Technology, Tehran, Iran.*
2. *Physics Department, Iran University of Science and Technology, Tehran, Iran.*
3. *Industrial Engineering Department, Iran University of Science and Technology, Tehran, Iran.*
4. *Physics Department, Iran University of Science and Technology, Tehran, Iran.*

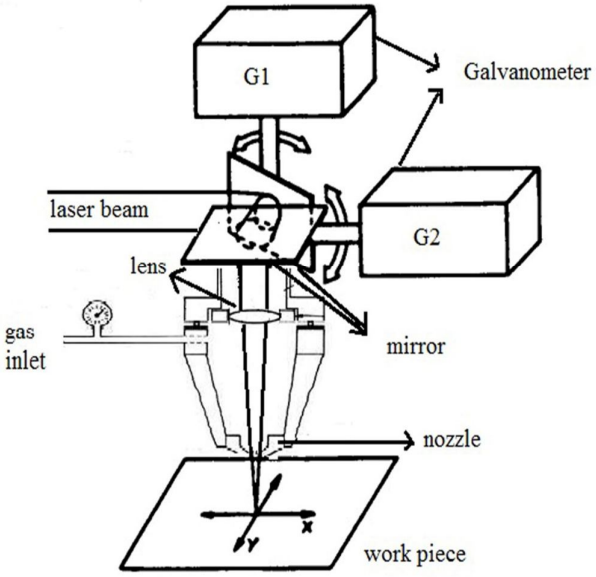

Fig. 1. Laser marking process

The effectiveness of a process or product can be expressed and evaluated using qualitative or quantitative characteristics. Design of Experiments (DOE) can be utilized as a systematic approach to modeling the output of a process, referred to as response variable, as a function of input or process variables. Factorial design is an efficient design that helps an experimenter evaluate the effects of two or more factors on the variable using Analysis of Variance (ANOVA) method. In the ANOVA, the null hypothesis that the means of the population from which random samples are collected are all identical is evaluated against the alternative hypothesis that at least one population has a different mean. In practice, the number of factors involved in an experiment easily increases, requiring an even more efficient factorial design. The 2^k factorial or 2^{k-p} fractional factorial designs known as screening designs helps experimenter evaluate the effects of several factors simultaneously while keeping the size of experiment to a manageable level [3]. Many industrial experiments are concerned with optimization of multiple responses. In multiple response optimization, it is desirable to find a setting of input factors which leads to simultaneous optimization of multiple responses. Taguchi's parameter design is a widely applied method for improving the quality based on a loss function. Generally, Taguchi's parameter design is based on a single response optimization [4]. In the field of experimental design, many authors focused on desirability function. This approach is popular in response surface methodology and is a common method for multiple response optimization as well [5-8].

In laser machining process, Hong et al. [9] used Taguchi method in the optimization of laser micro-engraving photo masks. They recommended the use of Taguchi method for optimization of micro-engraving of iron-oxide-coated glass. Mathew et al. [10] studied the laser cutting of Carbon Fiber Reinforced Plastic (CFRP). They used response surface methodology to optimize the process parameters. Ghoreishi [11] studied the effects of six parameters on the repeatability of drilled holes in laser drilling process through response surface methodology. The significant factors in this process were selected based on the analysis of variance method. Lee et al. [12] conducted a study on the optimization of laser welding parameters to seal an iodine-125 radioisotope seed into a titanium capsule. The effects of laser welding parameters on the melted length were analyzed using Taguchi and regression analysis methods. Kuar et al. [13] investigated the effects of several laser machining parameters on the Heat Affected Zone (HAZ), thickness, and taper of the microdrilled holes on alumina-aluminum composite using response surface methodology. Li et al. [14] reported on a study on optimal laser parameters for cutting Quad Flat No-Lead (QFN) packages using a $L_9(3^4)$ orthogonal array. The factors used in this experiment were laser current, laser frequency, and cutting speed and they were effective in laser cutting quality. Lin et al. [15]

studied the effects of feed speed ratio and laser output power on engraved depth and colour difference of Moso bamboo lamina. The values of engraved depth and color difference were predicted and estimated through regression analysis. Biswas et al. [16] studied the circularity of drilled hole that affected the quality of a drilled hole. The effect of several process parameters on hole circularity was analyzed through response surface methodology. Farahmand and Kovacevic [17] investigated laser cladding via a high-power direct diode laser as a heat source. They studied the effects of laser power, powder flow rate, and scanning speed on the clad-bead geometry and clad micro hardness. The response surface methodology and desirability function were used for optimization of cladding process. Mahamood et al. [18] studied the impact of laser power and scanning speed on the mechanical property of laser metal deposited titanium alloy. The full factorial experimental design was utilized to design and analyze the results. Kotadya and Pandya [19] analyzed the process parameters of laser cutting on surface characteristics of the cut section of stainless-steel sheets. Response surface methodology and ANOVA method were employed to analyze and optimize the surface roughness. The large number of parameters affecting the qualitative characteristics of laser machining processes requires a precise analysis. Avvari et al. [20] studied the optimization of hole characteristics during pulse Nd:YAG laser drilling of commercially pure titanium alloy. The effects of gas pressure, gas type, cutting speed, and nozzle diameter on material removal rate and hole tapper angle were analyzed. The Taguchi-based grey relation method was implemented to multi-objective optimization of characteristics.

The present paper aims to investigate the laser engraving qualitative characteristics of Al-SiC composite produced through ARB process.

1.1. Objectives of the study

In this paper, laser engraving, as a subset of laser machining and the most common technique in laser material processing, and design of experiments were used to identify the significant factors in laser engraving processes. Section 2 discusses the center point replicates method. Section 3 presents a basic discussion on desirability function. Section 4 elaborates the methodology used for experimentation. Section 5 introduces a real case study and the final section concludes this study.

2. Center Point Replicates Method

Center point replicates is a method that can be used to estimate the error sum of squares. The center point is a treatment where all factors are set exactly at the midpoint of the levels. Hence, the replicates at the center point provide an error of the estimate that is used to evaluate the hypothesis tests [3].

An appropriate model in this situation is the multiple linear regression model for 2^k factorial design. An additive model for the k factor $x_1, \dots, x_k$ is:

$$y = \beta_0 + \beta_1 x_1 + \cdots + \beta_k x_k + \varepsilon \quad (1)$$

where y is the regression coefficient, ε is the random error, and β_j is the response variable. In this model, the effect of j^{th} factor does not depend on the settings of the other $k-1$ factors. The additive model (1) can be written as:

$$y = \beta_0 + \sum_{j=1}^{k} \beta_j x_j + \varepsilon \quad (2)$$

The two-factor interaction model for 2^k factorial design is:

$$y = \beta_0 + \sum_{j=1}^{k} \beta_j x_j + \sum_{i=1}^{k-1} \sum_{j=i+1}^{k} \beta_{i,j} x_i x_j + \varepsilon \quad (3)$$

and saturated model for 2^k factorial design is:

$$y = \beta_0 + \sum_{i=1}^{k} \beta_i x_i + \sum_{i=1}^{k-1} \sum_{j=i+1}^{k} \beta_{i,j} x_i x_j + \sum_{i=1}^{k-2} \sum_{j=i+1}^{k-1} \sum_{l=i+1}^{k} \beta_{i,j,l} x_i x_j x_l + \cdots + \beta_{1.2\cdots k} x_1 x_2 \cdots x_k + \varepsilon \quad (4)$$

This model contains all possible k factor interaction effects and it fits the average response at each of the 2^k treatment combinations of the full factorial design. Of note, when the errors $\varepsilon_1, \cdots, \varepsilon_N$ are independently distributed with variance σ^2, the least squares estimation of a regression model provides an efficient estimator for the regression coefficients [21].

3. Desirability Function

The desirability function approach to simultaneous optimization of multiple response transforms the predicted values of the response variables into values within the interval [0,1], using three different desirability methods for three different optimization criteria of minimization, maximization, and target (nominal) values. A specific desirability function is assigned to each value of a response variable by three forms of this functions, based on the type of

optimization objective. The desirability function for a smaller and better type response is:

$$d_i(\tilde{y}_i) = \begin{cases} 0 & \text{if } y_i \geq B \\ (\frac{y_i - B}{A - B})^s & \text{if } A \leq y_i \leq B \\ 1 & \text{if } y_i < A \end{cases} \quad (5)$$

and for a larger the better type response is:

$$d_i(\tilde{y}_i) = \begin{cases} 0 & \text{if } y_i < A \\ (\frac{y_i - A}{B - A})^s & \text{if } A \leq y_i \leq B \\ 1 & \text{if } y_i > B \end{cases} \quad (6)$$

These functions are on the same scale at the points A (lower limit) and B (upper limit). The value of s is weight and is chosen to emphasize on the optimization objective. The overall desirability is characterized by the geometric mean of specific desirability functions [22].

4. Methodology

Three steps are recommended to fully investigate the laser engraving qualitative characteristics of Al-SiC composite using a 2^k factorial design.

Step 1: This step includes building an unreplicated 2^k factorial design for each of qualitative characteristics of Al-SiC composite. Running multiple replicates at center points provides an estimate of pure error.

Step 2: In this step, the saturated model for 2^k factorial design is used for hypothesis testing. The method of least squares applied in order to test the significance of the main and interaction effects. Then, a 3D visualization is done with the response surface plot.

Step 3: Finally, the desirability function is implemented for optimization of multiple responses based on hat-values of multiple linear regression model.

The qualityTools package in R software (version 3.3.0) was utilized to analyze the effect of laser engraving process parameters on the qualitative characteristics of Al-SiC composite produced through Accumulative Roll Bounding (ARB) process.

5. Experimental Planning Based On 2^k Design

Al-SiC is a metal-ceramic composite material which contains silicon carbide particles dispersed in a matrix of aluminum alloy. It enjoys the benefits of high thermal conductivity of metal and low Coefficient of Thermal Expansion (CTE) of ceramic. Given these features, Al-SiC is an appropriate composite for high technology thermal management [23]. Accumulative roll bounding process is a sever plastic deformation technique which has great advantages such as grain refinement and high strengthening of the materials. The ARB process is useful for practical applications since it is performed by the conventional rolling process. This process can be used for producing various metallic materials such as aluminum alloys [24].

The laser beam machining is an advanced manufacturing process in which a laser is directed towards the workpiece for machining. The laser engraving, as a subset of laser beam machining, is regarded as a practice of using laser to engrave anything on an object. This technique involves the use of neither link nor tool bits which contact the engraving surface [25].

The present paper aims to investigate the effect of laser engraving process parameters on the qualitative characteristics of Al-SiC composite produced using ARB process.

The studied qualitative characteristics consist of the function of assistant gas flow (x_1), distance between the surface of workpiece and beam focus location (x_2), pulse frequency (x_3), and pumping current (x_4), all considered at two levels. The amount of assistant gas flow varies from 6 to 12 lit/min; the distance between the surface of workpiece and beam focus location is 0.5 to 1.5 mm; the pulse frequency ranges from 2 to 4 kHz; and the pumping current varies from 14 to 17 Amp. Low factor settings are assigned a-1 and high values a+1.

A 16-run 2^k experimental design is performed by adding 6 center points in order to study the effect of input factors on depth (per μm), width (per μm), and contrast of engraved zone as response variables. The center points were assigned a 0 and considered to be 9, 1, 3, and 15.5, respectively. This study aims to achieve the optimal setting of input parameters to ensure maximization of depth (y_1), minimization of width (y_2), and maximization of contrast (y_3). Fig. 2 shows a schematic representation of the laser engraving process of Al- SiC composite.

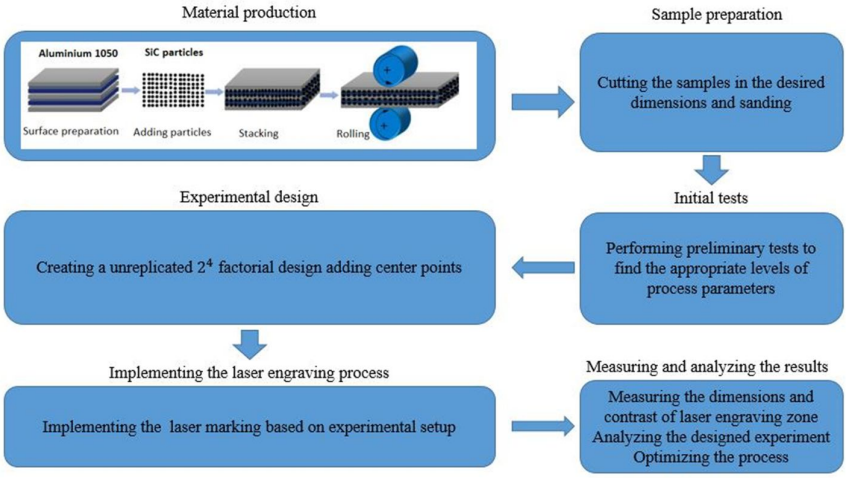

Fig. 2. Laser engraving process of Al-Sic composite

Table 1 shows the experimental setup for laser engraving qualitative characteristics of Al-Sic composite, using center point replicates method.

Tab. 1. Experimental setup for laser engraving qualitative characteristics of Al-Sic composite based on coded values

NO.	x_1	x_2	x_3	x_4	y_1	y_2	y_3
1	1	1	-1	-1	90.4	100.03	0.07
2	-1	-1	1	1	67.3	73.02	0.04
3	-1	-1	-1	1	106.4	144.6	0.12
4	-1	1	-1	-1	60.9	101.1	0.16
5	-1	1	1	1	54.9	83.2	0.11
6	0	0	0	0	97.7	99.2	0.05
7	0	0	0	0	103.6	109.6	0.06
8	1	-1	-1	-1	83.9	169	0.47
9	1	1	1	-1	113.2	81.4	0.02
10	-1	1	1	-1	106.8	83.7	0.11
11	1	1	-1	1	123.8	134.1	0.2
12	0	0	0	0	105.2	102.8	0.04
13	0	0	0	0	102.4	105.7	0.04
14	0	0	0	0	100.6	109.8	0.04
15	-1	-1	1	-1	106	116.8	0.18
16	1	-1	1	1	107.8	111.1	0.06
17	-1	1	-1	1	89.3	132.3	0.13
18	1	-1	-1	1	93.1	148.8	0.33
19	1	1	1	1	92.8	120.9	0.08
20	1	-1	1	-1	116.4	162.3	0.27
21	-1	-1	-1	-1	71.7	100.2	0.07
22	0	0	0	0	100.3	101.8	0.06

5.1. Data analysis

A saturated model with four main effects, six two-factor interactions, four three-factor interactions, and one four-factor interactions is fitted to each of qualitative characteristics separately. The results of full factorial analysis of the depth of engraved zone are shown in Table 2.

Tab. 2. Full factorial analysis for depth

Coefficients	Estimate	Std. Error	t-value	Pr(> |t|)
Intercept	95.2045	1.6888	56.375	2.09e-09
x_1	9.8813	1.9803	4.990	0.002477
x_2	-1.2812	1.9803	-0.647	0.541572
x_3	2.8563	1.9803	1.442	0.199297
x_4	-0.8687	1.9803	-0.439	0.676233
$x_1 : x_2$	3.6562	1.9803	1.846	0.114369
$x_1 : x_3$	2.0187	1.9803	1.019	0.347329

$x_1:x_4$	-2.4438	1.9803	1.234	0.263325
$x_2:x_3$	2.5687	1.9803	1.297	0.242215
$x_2:x_4$	-0.4438	1.9803	-0.224	0.830126
$x_3:x_4$	-14.0813	1.9803	-7.111	0.000389
$x_1:x_2:x_3$	-4.4812	1.9803	-2.263	0.064287
$x_1:x_2:x_4$	1.9938	1.9803	1.007	0.352890
$x_1:x_3:x_3$	5.1313	1.9803	2.591	0.041146
$x_2:x_3:x_4$	-2.6812	1.9803	1.354	0.224514
$x_1:x_2:x_3:x_4$	-1.8188	1.9803	-0.918	0.393813

According to Table 2, one-main effect assistant gas flow, two-interaction effect between pulse frequency and pumping current, three-interaction effect between assistant gas flow, distance, and pulse frequency, and three-interaction effect between assistant gas flow, pulse frequency, and pumping current are significant.

The main effect plots are the graphs of depth averages at the levels of four factors as shown in Fig. 3. The gas flow and pulse frequency are factors that have an increasing effect on depth. The distance and pumping current are factors that have a decreasing effect on depth.

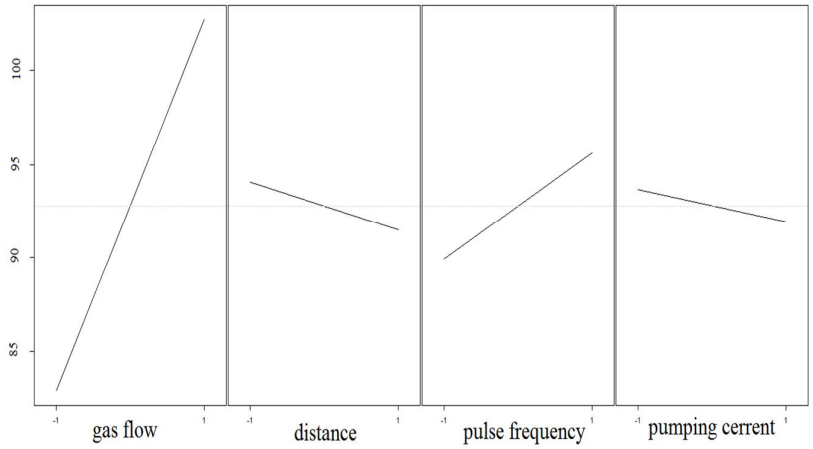

Fig. 3. Main effects plots of input factors for the depth

Decreasing the effect of pumping current on depth may be physically disputed. Hence, the two-interaction plots were employed for a more precise analysis. The two-way interaction affects the depth of engraved zone, as shown in Fig. 4.

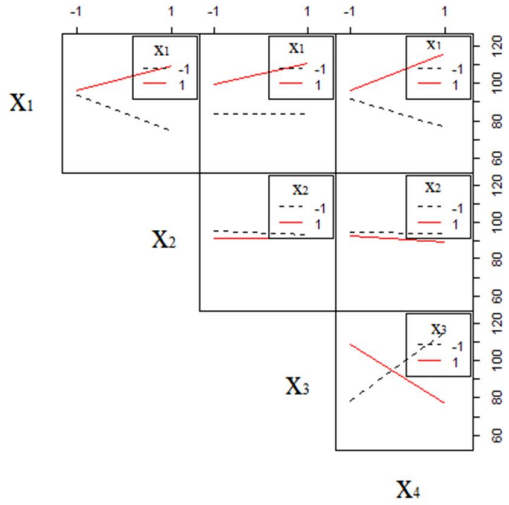

Fig. 4. Two-interaction plots for the depth

According to Fig 4, at the high level of assistant gas flow and low level of pulse frequency, the pumping current has an increasing effect on the depth of engraved zone. With increasing the pumping current, the power of laser increases linearly. Increasing the laser power leads to an increase in temperature and amount of material removal.

Fig. 5 (a,b) shows the response surface for depth of engraved zone versus significant two-interaction effects of pulse frequency and pumping current.

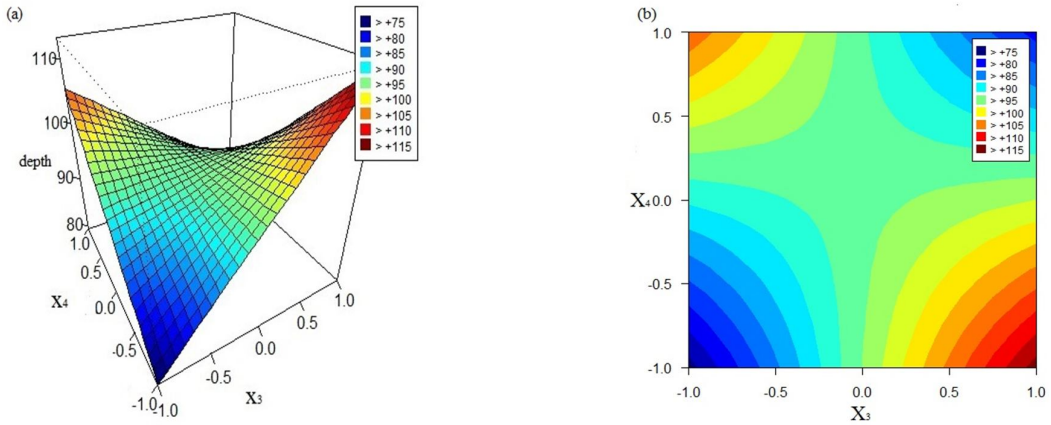

Fig. 5. A Response surface plot, **B** contour plot for depth versus pulse frequency and pumping current

Based on Figure 5 (a,b), the response surface plot contains saddle point. This point is of approximately 3 kHz pulse frequency and 15.5 A pumping current. This saddle point shows that a simultaneously increase in the pulse frequency and pumping current leads to an increase and then, a decrease in the depth of engraved zone.

The results of full factorial analysis for width of engraved zone are shown in Table 3.

Tab. 3. Full factorial analysis for width

Coefficients	Estimate	Std. Error	t-value	P-value
Intercept	113.24773	2.26910	49.909	4.34e-09
x_1	12.04437	2.66075	4.527	0.00399
x_2	-11.81812	2.66075	4.442	0.00437
x_3	-12.35687	2.66075	-4.644	0.00353
x_4	2.09312	2.66075	0.787	0.46141
$x_1:x_2$	-7.52813	2.66075	-2.829	0.02998
$x_1:x_3$	2.82812	2.66075	1.063	0.32872
$x_1:x_4$	0.06563	2.66075	0.025	0.98112
$x_2:x_3$	-1.82187	2.66075	-0.685	0.51908
$x_2:x_4$	10.94063	2.66075	4.112	0.00627
$x_3:x_4$	-9.09063	2.66075	-3.417	0.01420
$x_1:x_2:x_3$	1.50563	2.66075	0.566	0.59200
$x_1:x_2:x_4$	7.18063	2.66075	2.699	0.03564
$x_1:x_3:x_4$	5.89437	2.66075	2.215	0.06864
$x_2:x_3:x_4$	5.80688	2.66075	2.182	0.07182
$x_1:x_2:x_3:x_4$	-1.25313	2.66075	-0.471	0.65430

As shown in Table 3, three main effects (assistant gas flow, distance, and pulse frequency), two-way interaction effect between assistant gas flow and distance, two-way interaction effect between distance and pumping current, two-way interaction effect between pulse frequency and pumping current, three-way interaction effect between assistant gas flow, distance, and pumping current, three-way interaction effect between assistant gas flow, pulse frequency, and pumping current, and three-way interaction effect between distance, pulse frequency, and pumping current are significant. The main effect of input factors on width are shown in Fig. 6. The gas flow and pumping current are factors that have an increasing effect on width.

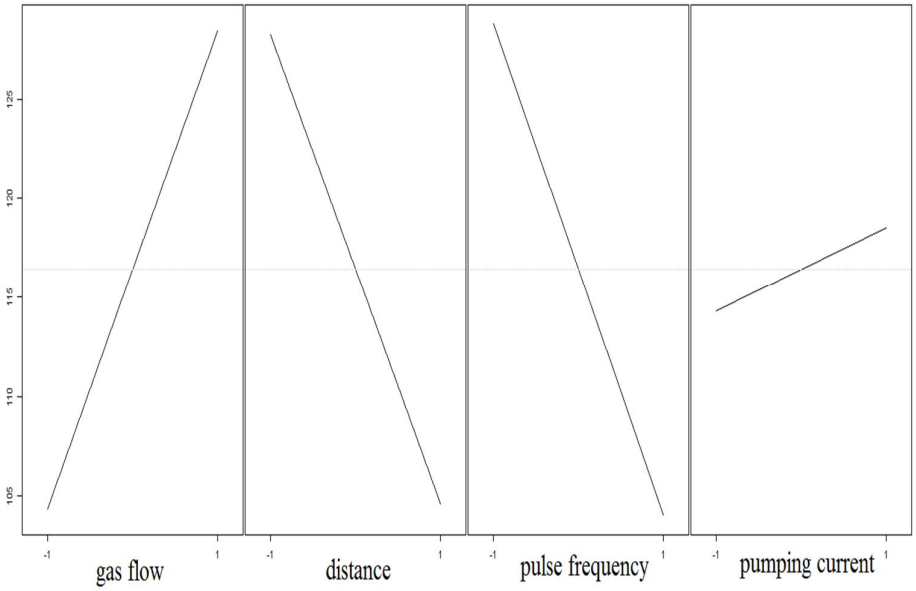

Fig. 6. Main effects plots of input factors for the width

The two-way interaction effects for width of engraved zone are shown in Fig. 7.

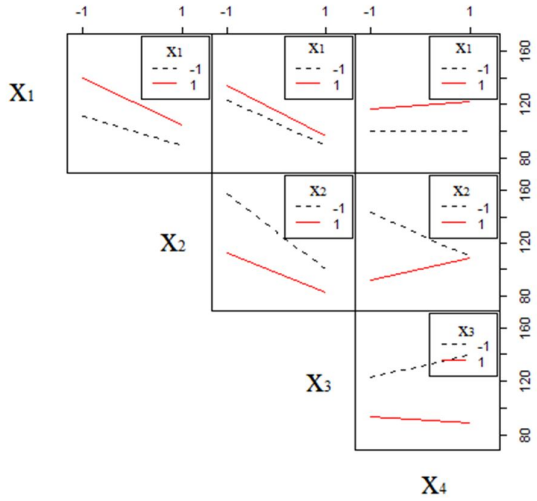

Fig. 7. Two-way interaction plots for the width

Fig. 8 (a,b) shows the response surface for width of engraved zone versus significant two-interaction effects of assistant gas flow and distance.

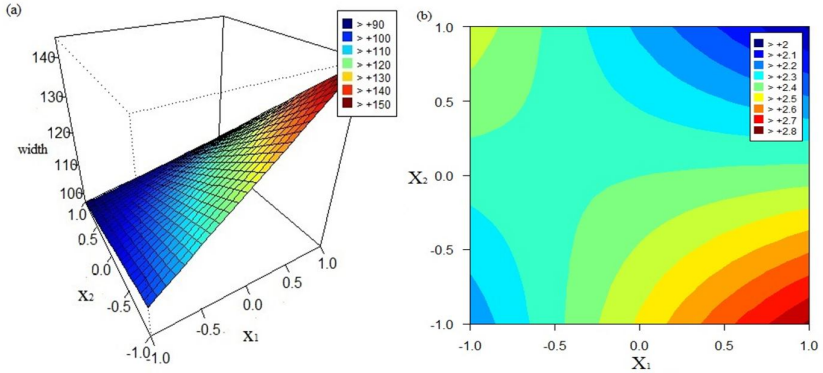

Fig. 8. A Response surface plot, **B** contour plot for width versus assistant gas flow and distance

The response surface is a twisted plane, and the true optimum is a point with minimum width. This point is quite close to 6 lit/min assistant gas flow and 1.5 mm distance between surface of workpiece and beam focus location.

Fig. 9 (a,b) shows the response surface for width of engraved zone versus significant two-interaction effects of distance and pumping current.

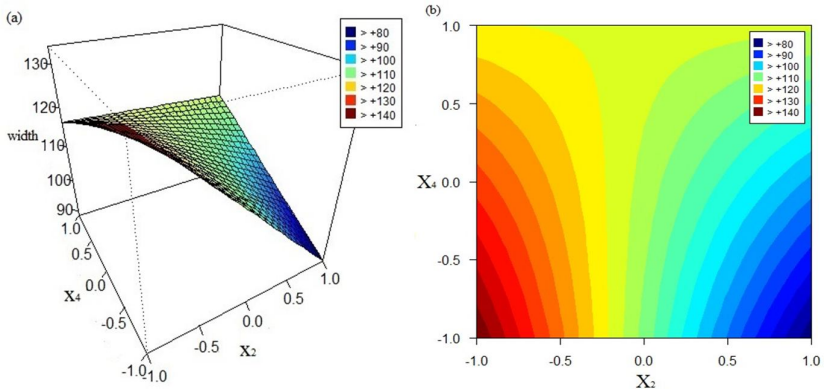

Fig. 9. A Response surface plot, **B** contour plot for width versus distance and pumping current

The optimum point is quite close to 1.5 mm, showing the distance between surface of workpiece and beam focus location, with the pumping current of 14 A and minimum width.

A saturated model was firstly adjusted to the original data set of contrast. Shapiro-Walk statistics indicated lack of normality in data behavior. Box-Cox transformation was used to achieve a normalizing transformation of a positive-valued response variable of contrast. The results of full factorial analysis for the transformed contrast of engraved zone are shown in Table 4.

Tab. 4. Full factorial analysis for transformed contrast

Coefficients	Estimate	Std. Error	t-value	Pr(> |t|)
Intercept	2.399500	0.095476	25.132	2.61e-07
x_1	0.027103	0.111955	0.242	0.8168
x_2	-0.111584	0.111955	-0.997	0.3574
x_3	-0.187002	0.111955	-1.670	0.1459
x_4	-0.010135	0.111955	-0.091	0.9308
$x_1:x_2$	-0.220978	0.111955	-1.974	0.0958
$x_1:x_3$	-0.131994	0.111955	-1.179	0.2830
$x_1:x_4$	-0.020866	0.111955	-0.186	0.8583
$x_2:x_3$	0.076269	0.111955	0.681	0.5211
$x_2:x_4$	0.186737	0.111955	1.668	0.1464
$x_3:x_4$	-0.088953	0.111955	-0.795	0.4571
$x_1:x_2:x_3$	-0.001024	0.111955	-0.009	0.9930
$x_1:x_2:x_4$	0.128460	0.111955	1.147	0.2949
$x_1:x_3:x_4$	0.048210	0.111955	0.431	0.6818
$x_2:x_3:x_4$	0.146417	0.111955	1.308	0.2388
$x_1:x_2:x_3:x_4$	-0.018873	0.111955	-0.169	0.8717

According to Table 4, the two-way interaction effect between the assistant gas flow and distance is significant. The main effect of input factors on transformed contrast are shown in Fig. 10. The assistant gas flow has an increasing effect on the contrast and distance; on the contrary, pulse frequency and pumping current are factors that have a decreasing effect on contrast.

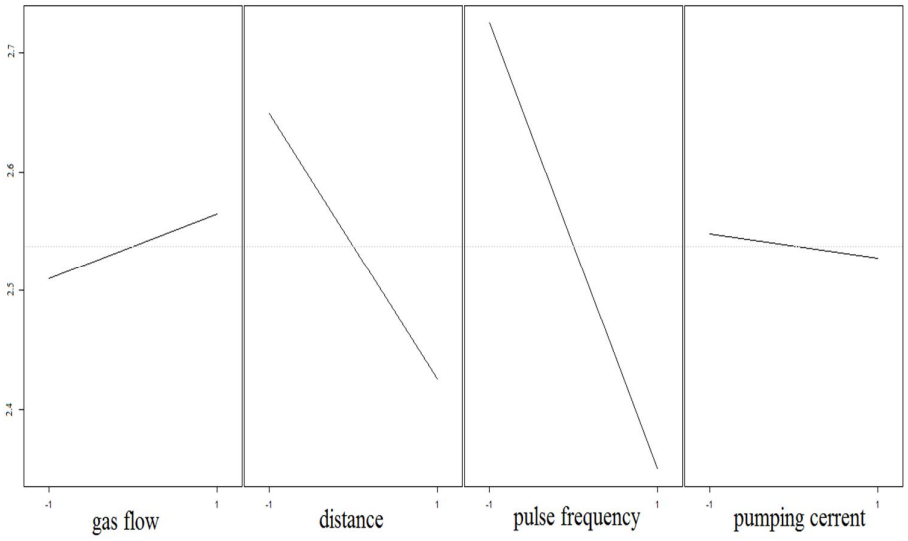

Fig. 10. Main effect plots of input factors for the contrast

The two-way interaction effects for contrast of engraved zone are shown in Fig. 11.

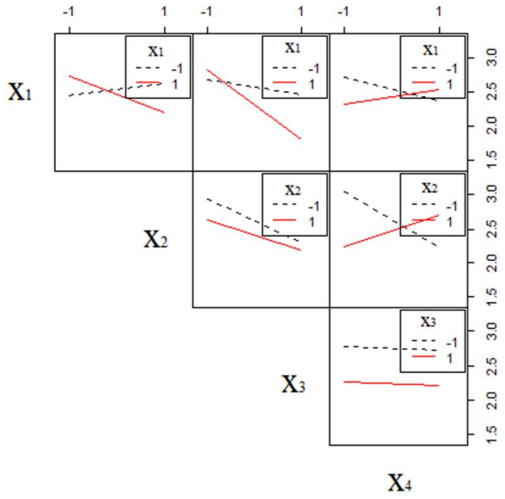

Fig. 11. Two-way interaction plots for the contrast

Fig. 12 (a,b) shows the response surface for contrast of engraved zone versus significant two-interaction effects of assistant gas flow and distance.

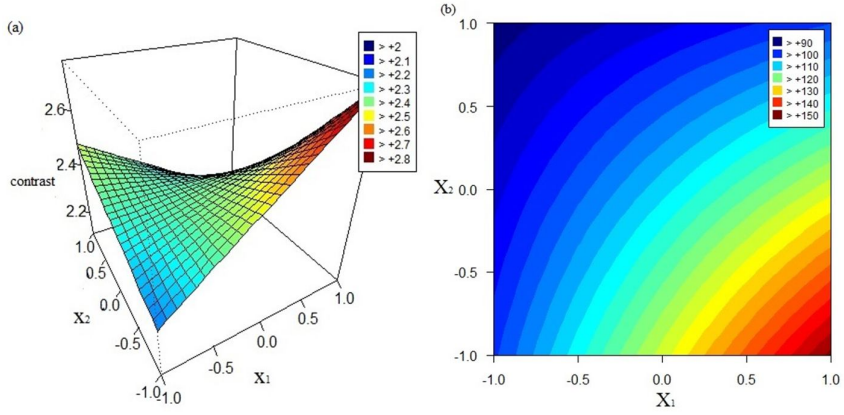

Fig. 12. A Response surface plot, **B** contour plot for contrast versus assistant gas flow and distance

Based on Figure 12 (a,b) the response surface plot contains saddle point. This point is very near 9 lit/min assistant gas flow and 1 mm distance between surface of workpiece and beam focus location. The saddle point argues that increasing in the assistant gas flow simultaneously with decreasing in the distance leads to increasing in the contrast of engraved zone.

The desirability function with the weight value (w) of 1 was used for optimization of multiple responses based on hat-values of multiple linear regression models.

The joint desirability is maximization of depth, minimization of width, and maximization of contrast. Fig. 13 shows three primary desirability functions. Panels of depth and contrast show a larger and better and panel of width shows a smaller and better desirability function.

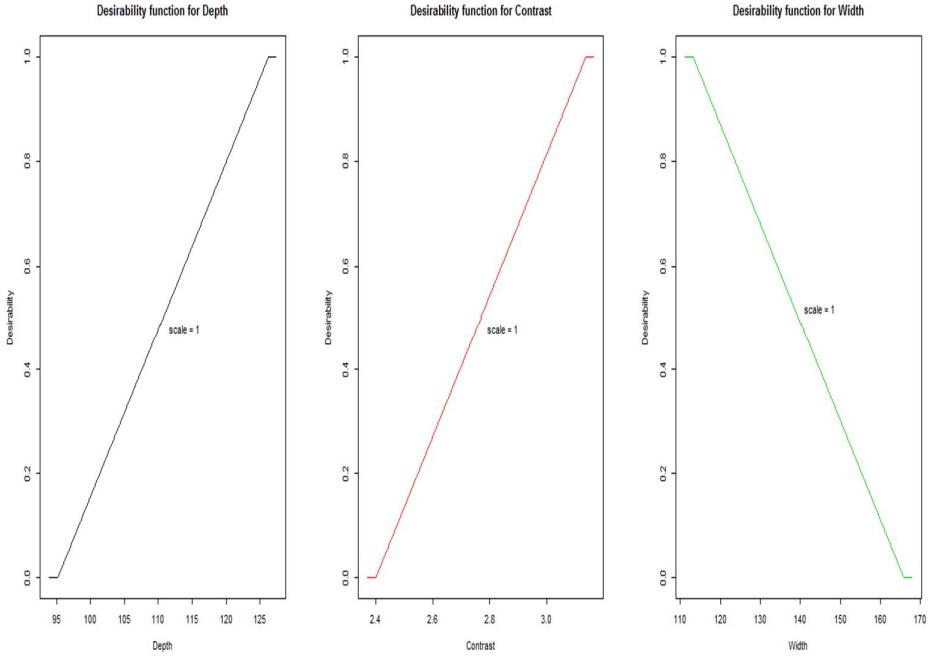

Fig. 13. Desirability functions for Al-SiC composite qualitative characteristics

The optimal setting for each input factor is shown in Table 5.

Tab. 5. Optimal setting of input factors

	gas flow	distance	Pulse frequency	Pumping current
Coded value	-1	1	1	0
Real value	6	1.5	4	15

The predicted responses for the optimal setting are shown in Table 6.

Tab. 6. Predicted responses

	Depth (μm)	Width (μm)	Contrast
Responses	107.331	126.93	0.01
Desirabilities	0.391	0.74	0.453

Distancing from the beam focus location shows a decrease in all three qualitative characteristics while gas flow has an increasing effect on all three qualitative characteristics.

Finally, ten additional experiments based on the optimal setting were conducted and the average of the measured responses were used for validation. The experimental results of depth, width, and contrast of engraved zone were 109.8 μm , 125.6 μm , and 0.018, respectively. The average of the responses is quite close to the predicted responses through desirability function. The percentage of prediction errors for the depth, width, and contrast are 0.02, 0.01, and 0.44, respectively.

6. Conclusion and Future Work

In this study, the effect of assistant gas flow, distance between surface of workpiece and beam focus location, pulse frequency, and pumping current on the qualitative characteristics of Al-SiC composite namely depth, width, and contrast of engraved zone is investigated. Different plots of the residuals from a fitted model provided information on the adequacy of different aspects of the model. Analysis indicates that assistant gas provides better (more transferred energy to the samples) interaction between laser and sample that leads to the dispersion of the resulting vapors and increases the depth and width of the engraved zone. With increasing the assistant gas, the contrast of engraved zone increases because it prevents oxidation of sample surface. Increasing the pumping current increases the laser average power linearly. By increasing the laser average power, both transferred energy and evaporation increase. Thus, with increasing pumping current, the depth and with of the engraved zone increase. Fig. 14 shows the microscopic image of samples after laser engraving process.

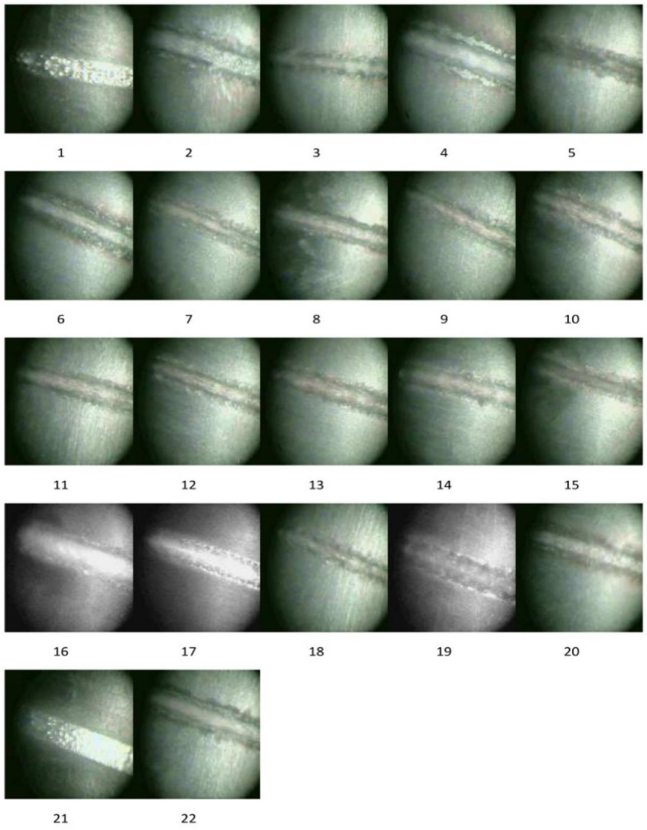

Fig. 14. Microscopic image of samples after laser engraving process

References

[1] Bagger, C. and Olsen, F.O. "Pulsed mode laser cutting of sheets for tailored blanks." Journal of Materials Processing Technology Vol. 115, No. 1, (2001), pp. 131-135.

[2] Kleine, K.F., Whitney, B. and Watkins, K.G. "Use of fiber lasers for micro cutting applications in the medical device industry." 21st International Congress on Applications of Lasers and Electro-Optics, Scottsdale. (2002).

[3] Montgomery, D. C. "Design and Analysis of Experiments." (2009).

[4] Liao, H.C. and Chen, Y.K. "Optimizing multi-response problem in the Taguchi method by DEA based ranking method." International Journal of Quality & Reliability Management Vol. 19, No. 7, (2002), pp. 825-837.

[5] Rueda, M.E., Sarabia, L.A., Herrero, A. and Ortiz, M.C. "Optimisation of a flow injection system with electrochemical detection using the desirability function:

application to the determination of hydroquinone in cosmetics." Analytica Chimica Acta Vol. 479, No. 2, (2003), pp. 173-184.

[6] Li, J., Ma, C., Ma, Y., Li, Y., Zhou, W. and Xu, P. "Medium optimization by combination of response surface methodology and desirability function: an application in glutamine production." Applied microbiology and biotechnology Vol. 74, No. 3, (2007), pp. 563-571.

[7] Aggarwal, A., Singh, H., Kumar, P. and Singh, M. "Optimization of multiple quality characteristics for CNC turning under cryogenic cutting environment using desirability function." Journal of materials processing technology Vol. 205, No. 1-3 (2008), pp. 42-50.

[8] Senthil, P., Selvaraj, T., Kannan, G. and Jeyapaul, R. "Multi response optimisation of turning operation parameters on Al-Cu/TiB 2 in-situ metal matrix composites using desirability function." International Journal of Manufacturing Technology and Management Vol. 25, No. 1-3, (2012), pp. 1-18.

[9] Hong, C.Y., Long, C.W. and Chung, T.S. "Calculation of optical parameters in laser engraving of photomasks." (1995).

[10] Mathew, J., Goswami, G.L., Ramakrishnan, N. and Naik, N.K. "Parametric studies on pulsed Nd: YAG laser cutting of carbon fibre reinforced plastic composites." Journal of Materials Processing Technology Vol. 89, (1999), pp. 198-203.

[11] Ghoreishi, M. "Statistical analysis of repeatability in laser percussion drilling." The International Journal of Advanced Manufacturing Technology Vol. 29, No. 1, (2006), pp. 70-78.

[12] Lee, H.K., Han, H.S., Son, K.J. and Hong, S.B. "Optimization of Nd: YAG laser welding parameters for sealing small titanium tube ends." Materials Science and Engineering: A Vol. 415, No. 1, (2006), pp. 149-155.

[13] Kuar, A.S., Paul, G. and Mitra, S. "Nd: YAG laser micromachining of alumina–aluminium interpenetrating phase composite using response surface methodology." International Journal of Machining and Machinability of Materials Vol. 1, No. 4, (2006), pp. 432-444.

[14] Li, C.H., Tsai, M.J. and Yang, C.D. "Study of optimal laser parameters for cutting QFN packages by Taguchi's matrix method." Optics & Laser Technology Vol. 39, No. 4, (2007), pp. 786-795.

[15] Lin, C.J., Wang, Y.C., Lin, L.D., Chiou, C.R., Wang, Y.N. and Tsai, M.J. "Effects of feed speed ratio and laser power on engraved depth and color difference of Moso bamboo lamina." journal of materials processing technology Vol. 198, No. 1, (2008), pp. 419-425.

[16] Biswas, R., Kuar, A.S., Biswas, S.K. and Mitra, S. "Characterization of hole circularity in pulsed Nd: YAG laser micro-drilling of TiN–Al 2 O 3 composites." The International Journal of Advanced Manufacturing Technology Vol. 51, No. 9, (2010), pp. 983-994.

[17] Farahmand, P. and Kovacevic, R. "Parametric study and multi-criteria optimization in laser cladding by a high power direct diode laser." Lasers in Manufacturing and Materials Processing Vol. 1, No. 1-4, (2014), pp. 1-20.

[18] Mahamood, R.M., Akinlabi, E.T. and Akinlabi, S. "Laser power and scanning speed influence on the mechanical property of laser metal deposited titanium-alloy." Lasers in Manufacturing and Materials Processing Vol. 2, No. 1, (2015), pp. 43-55.

[19] Kotadiya, D.J. and Pandya, D.H. "Parametric Analysis of Laser Machining with Response Surface Method on SS-304." Procedia Technology Vol. 23, (2016), pp. 376-382.

[20] Avvari, M., Manjaiah, M., Able, M., Laubscher, R.F. and Raghavendra, K. "Optimization of Hole Characteristics During Pulse Nd: YAG Laser Drilling of Commercially Pure Titanium Alloy." Lasers in Manufacturing and Materials Processing (2017), pp. 1-16.

[21] Mee, R. A comprehensive guide to factorial two-level experimentation. Springer Science & Business Media, (2009).

[22] Derringer, G. and Suich, R. "Simultaneous optimization of several response variables." Journal of quality technology Vol. 12, No. 4, (1980), pp. 214-219.

[23] Occhionero, M.A., Hay, R.A., Adams, R.W. and Fennessy, K.P. "Aluminum silicon carbide (AlSiC) for cost-effective thermal management and functional microelectronic packaging design solutions." 12th European Microelectronics and Packaging Conference. Vol. 8, (1999).

[24] Lee, S.H. and Lee, S.R. "Fabrication And Mechanical Properties Of A Nanostructured Complex Aluminum Alloy By Three-Layer Stack Accumulative Roll-Bonding." Archives of Metallurgy and Materials Vol. 60, No. 2, (2015), pp. 1195-1198.

[25] Peter, J., Doloi, B. and Bhattacharyya, B. "Optimization of Nd: YAG Laser Marking of Alumina Ceramic Using RSM And ANN." AIP Conference Proceedings. Vol. 1315, No. 1, (2011).

Follow This Article at The Following Site:

Noorossana R, Shayganmanesh M, Pazhuheian F, Rahimi M H. Investigation of Laser Engraving Qualitative Characteristics of Al- SiC Composite Using Design of Experiments. IJIEPR. 2020; 31 (3) :409-422
URL: http://ijiepr.iust.ac.ir/article-1-828-en.html